Mon. Not. R. Astron. Soc. **411,** 627–634 (2011) doi:10.1111/j.1365-2966.2010.17708.x

Stellar population gradients from cosmological simulations: dependence on mass and environment in local galaxies

C. Tortora,[1⋆] A. D. Romeo,[2] N. R. Napolitano,[3] V. Antonuccio-Delogu,[4,5] A. Meza,[2] J. Sommer-Larsen[6,7,8] and M. Capaccioli[9,10]

[1] *Institut für Theoretische Physik, Universität Zürich, Winterthurerstrasse 190, CH-8057 Zürich, Switzerland*
[2] *Departamento de Ciencias Fisicas, Universidad Andres Bello, Av. Republica 220, Santiago, Chile*
[3] *INAF – Osservatorio Astronomico di Capodimonte, Salita Moiariello 16, I-80131 Napoli, Italy*
[4] *INAF – Osservatorio Astrofisico di Catania, Via S. Sofia 78, I-95123 Catania, Italy*
[5] *Scuola Superiore di Catania, Via San Nullo 5/i, 95123 Catania, Italy*
[6] *Excellence Cluster Universe, Technische Universität München, Boltzmannstr. 2, D-85748 Garching bei München, Germany*
[7] *Dark Cosmology Centre, Niels Bohr Institute, University of Copenhagen, Juliane Maries Vej 30, DK-2100 Copenhagen, Denmark*
[8] *Marie Kruses Skole, Stavnsholtvej 29–31, DK-3520 Farum, Denmark*
[9] *Dipartimento di Scienze Fisiche, Università di Napoli Federico II, Compl. Univ. Monte S. Angelo, 80126 Napoli, Italy*
[10] *MECENAS, Università di Napoli Federico II, I-80134 Napoli and Università di Bari, I-70126 Bari, Italy*

Accepted 2010 September 13. Received 2010 August 1; in original form 2010 June 23

ABSTRACT

The age and metallicity gradients for a sample of group and cluster galaxies from *N*-body+hydrodynamical simulation are analysed in terms of galaxy stellar mass. Dwarf galaxies show null age gradient with a tail of high and positive values for systems in groups and cluster outskirts. Massive systems have generally zero-age gradients which turn to positive for the most massive ones. Metallicity gradients are distributed around zero in dwarf galaxies and become more negative with mass; massive galaxies have steeper negative metallicity gradients, but the trend flattens with mass. In particular, fossil groups are characterized by a tighter distribution of both age and metallicity gradients. We find a good agreement with both local observations and independent simulations. Interestingly, our results suggest that environment differently affects the gradients at low and high masses. The results are also discussed in terms of the central age and metallicity, as well as the total colour, specific star formation and velocity dispersion.

Key words: galaxies: elliptical and lenticular, cD – galaxies: evolution – galaxies: general.

1 INTRODUCTION

Radial profiles of colours, ages and metallicities of stellar populations have been shown to be efficient tools to discriminate among different galaxy formation scenarios across a wide range of masses and environments. Earlier observational works were unable to assess the dependence of gradients on mass, mainly because of the limited samples studied (Peletier et al. 1990a, b; Davies, Sadler & Peletier 1993; Kobayashi & Arimoto 1999; Tamura & Ohta 2003; La Barbera et al. 2005). Only recently, trends of gradients with mass have been more firmly assessed (e.g. Forbes, Sánchez-Blázquez & Proctor 2005), pointing towards different physical mechanisms forging the behaviour of more and less massive galaxies (Spolaor et al. 2009; Rawle, Smith & Lucey 2010; Tortora et al. 2010, hereafter T+10). However, the dependence of the stellar population gradients on environment is still controversial (Tamura et al. 2000; Tamura & Ohta 2000, 2003), although it might have a non-marginal role (e.g. La Barbera et al. 2005).

Simulations of galaxy formation are the ideal tool to interpret observations in terms of the underlying physical mechanisms driving the evolutive processes of galaxies in various environments and a large mass range. For instance, in T+10 we have compared the stellar population (age and metallicity) gradients of a wide sample of local galaxies extracted from the Sloan Digital Sky Survey, with a number of literature simulations (of both monolithically collapsing systems and merger remnants). We have confirmed the metallicity as the main factor in shaping the colour gradient as a function of mass. However, age gradients are still important, particularly for younger galaxies. We have shown that less massive systems, which are unlikely to get assembled by merging, have experienced a simple monolithic collapse, resulting into a negative and steep metallicity gradient (e.g. Larson 1974, 1975; Carlberg 1984) which decreases with mass (Kawata & Gibson 2003; Pipino et al. 2010). Supernovae (SNe) feedback is strong in this mass regime, reaching its maximum efficiency in the lowest mass systems and this contributes to produce such negative gradients (Pipino, D'Ercole & Matteucci 2008). On the higher mass side instead, the trend with mass is inverted, demanding the contribution of strong joint effect

⋆E-mail: ctortora@physik.uzh.ch

of merging and active galactic nuclei (AGN) feedback (Bekki & Shioya 1999; Kobayashi 2004; Sijacki et al. 2007; Hopkins et al. 2009). In spite of these results, recently Pipino et al. (2010) have reproduced the flattening of metallicity gradients in massive systems within a monolithic scenario of galaxy formation, pointing to a fundamental role of star formation efficiency in shaping the trend with mass.

In the present paper we will use the TREESPH N-body+hydrodynamical simulations described in Romeo et al. (2006, 2008, hereafter R+06 and R+08) to derive the profiles of both age and metallicity inside the galaxies and discuss them as a function of stellar mass and environment. This smoothed particle hydrodynamics (SPH) simulation has some advantages when compared with either semi-analytical models (SAMs) or pure hydrodynamical simulations of individual objects. In general SAMs make use of large-scale N-body simulations and rely upon different sets of assumptions and approximations (e.g. dark matter haloes are spherically symmetric and infalling gas is shock heated to the virial temperature of the halo) that depend on many interconnected and variable parameters [such as star formation and feedback efficiency or initial mass function (IMF)]. In this scheme, the evolution of galaxies is adjusted on top of the pure collisionless dark matter (DM) haloes by means of merger trees and models of synthetic colours. On the other hand, SPH simulations contain fewer simplifying assumptions (as e.g. no restrictions on halo geometry), but have to restrict themselves on smaller scales (namely galactic) in order to maintain a high resolution, resulting in a more limited dynamical range. However, in terms of gas cooling both approaches are confirmed to give similar results (Benson et al. 2001; Helly et al. 2003). Our approach roughly lies in between, since the formation of galaxies is followed *ab initio* within a large cosmological volume, thus accounting for their interaction with a large-scale environment. At the same time, it allows for describing in a self-consistent way the mutual cycle between intergalactic medium (IGM), star formation and stellar feedback at the cluster scale, by means of the baryonic physics implemented in the hydrodynamical code, in particular the chemical enrichment of the gas surrounding galaxies (for details, see R+06). This is though attained at expenses of the final stellar resolution that cannot reach the level of either pure N-body simulations used in SAMs, nor of the single-object hydrodynamical simulations at smaller scale. In this paper then we will test our SPH simulations against both observations and models, with the caveat of latter's different resolution: e.g. those of gas-rich mergers between discs by Bekki & Shioya (1999) and Hopkins et al. (2009), or the cosmological simulations including a chemodynamical model by Kawata & Gibson (2003).

In Section 2 we will present the simulation set-up and the fitting procedure adopted to recover the gradients; systematics in the fitting procedure and simulation resolution are analysed in Appendix A. In Sections 3 and 4 the trends with mass and environment are analysed and we give an interpretation of the physical processes, while the conclusions are drawn in Section 5.

2 SIMULATION SET-UP

We have extracted simulated galaxies from the SPH simulations in R+06 of two clusters of temperatures $T \sim 3$ (C1) and 6 keV (C2) and 12 groups ($T \sim 1.5$ keV), four of which are fossil. They were drawn and resimulated from a DM-only cosmological simulation run with the code FLY (Antonuccio-Delogu et al. 2003), for a standard flat Λ cold dark matter (ΛCDM) cosmological model ($h = 0.7, \Omega_{\rm m} = 0.3, \sigma_8 = 0.9$) with $150\,h^{-1}$ Mpc box length. When resimulating with the hydrocode, baryonic particles were 'added' to the original DM ones, which were split according to a chosen baryon fraction $f_{\rm b} = 0.12$.

Galaxies are composed by $N_{\rm par}$ star particles bound to the DM halo; each star particle represents a single stellar population (SSP) of total stellar mass corresponding to the stellar mass resolution ($M_{\star,\rm SSP}$) of the simulation. This is $M_{\star,\rm SSP} = 3.1 \times 10^7\,h^{-1}$ for groups and C1, while $M_{\star,\rm SSP} = 25 \times 10^7\,h^{-1}$ for C2. The total luminosity and mass for each galaxy is defined as the sum of the luminosities and masses of their $N_{\rm par}$ star particles. The individual stellar masses are distributed according to an Arimoto & Yoshii (1987, hereafter AY) IMF; each of these SSPs is characterized by its age and metallicity (Z), from which luminosities are computed by mass-weighted integration of the Padova isochrones. The 'standard' superwind model for SN is adopted, i.e. a prescription for SN feedback in which 70 per cent of the energy feedback from Type II SN goes into driving galactic superwinds (see R+06 for more details). Although AGN feedback is not taken into account in this simulation, R+08 has shown that the colour properties of galaxies are fairly good reproduced; however, AGNs would play a major role only in high-mass systems.

Because of the galactic winds expelling baryons out into the IGM, lower mass galaxies have a higher fraction of DM over stars (and gas), which also results in a low absolute number of star particles. Throughout this paper we will only deal with the stellar component, willing to remain as much as consistent with the approach followed in the observations. For this reason it is important to determine a lower limit to the number of star particles, in order to avoid systems whose stellar component is not sufficiently resolved.

We have originally applied a completeness limit in stellar mass of $\log M_*/{\rm M}_\odot > 9.5$, but to be more conservative we have only retained those systems having $N_{\rm par} > 80$. We are left with a sample including 32 galaxies from the two clusters and 97 from the 12 groups, at $z = 0$. The systematics in the galaxies with a lower number of particles will be discussed in Appendix A2, where we also show how the results could change when systems with $N_{\rm par} \leq 80$ were included.

Brightest central galaxies (BCGs) are excluded from this analysis, since their diffuse envelope mixing with the intracluster light makes difficult to fit a reliable luminosity profile on the basis of the galaxy-bound star particles only.

For a given stellar population parameter X (= age, Z), we will assume the radial variation as $\log X\,(R) = a_X + b_X \log R$, and define the X gradient as the angular coefficient $b_X = \nabla_X = [\delta(\log X)/(\delta \log R)]$. For convenience, we adopt as central quantity the value of $\log X$ at $R = 1$ kpc, i.e. the intercept a_X. By definition, if the gradient is positive, i.e. $\nabla_X > 0$, then X is lower in the central regions, while X decreases as a function of R when the gradient is negative, i.e. $\nabla_X < 0$.

The centre of the galaxy is defined as the median of the positions of all the star particles. The fit is made after having discarded those particles with age and metallicities $>3\sigma$ away from the median (see Appendix A1 for further details). To take into account disturbed galaxy shapes, we performed the log–log fit on three projected orthogonal planes and took the median of the parameters to obtain the final gradient values.

3 RESULTS

We show the age and metallicity gradients for groups and clusters as a function of stellar mass in Fig. 1. As shown in the upper panels of this figure, on average, low-mass systems have null age gradients and very shallow (either negative or positive) metallicity

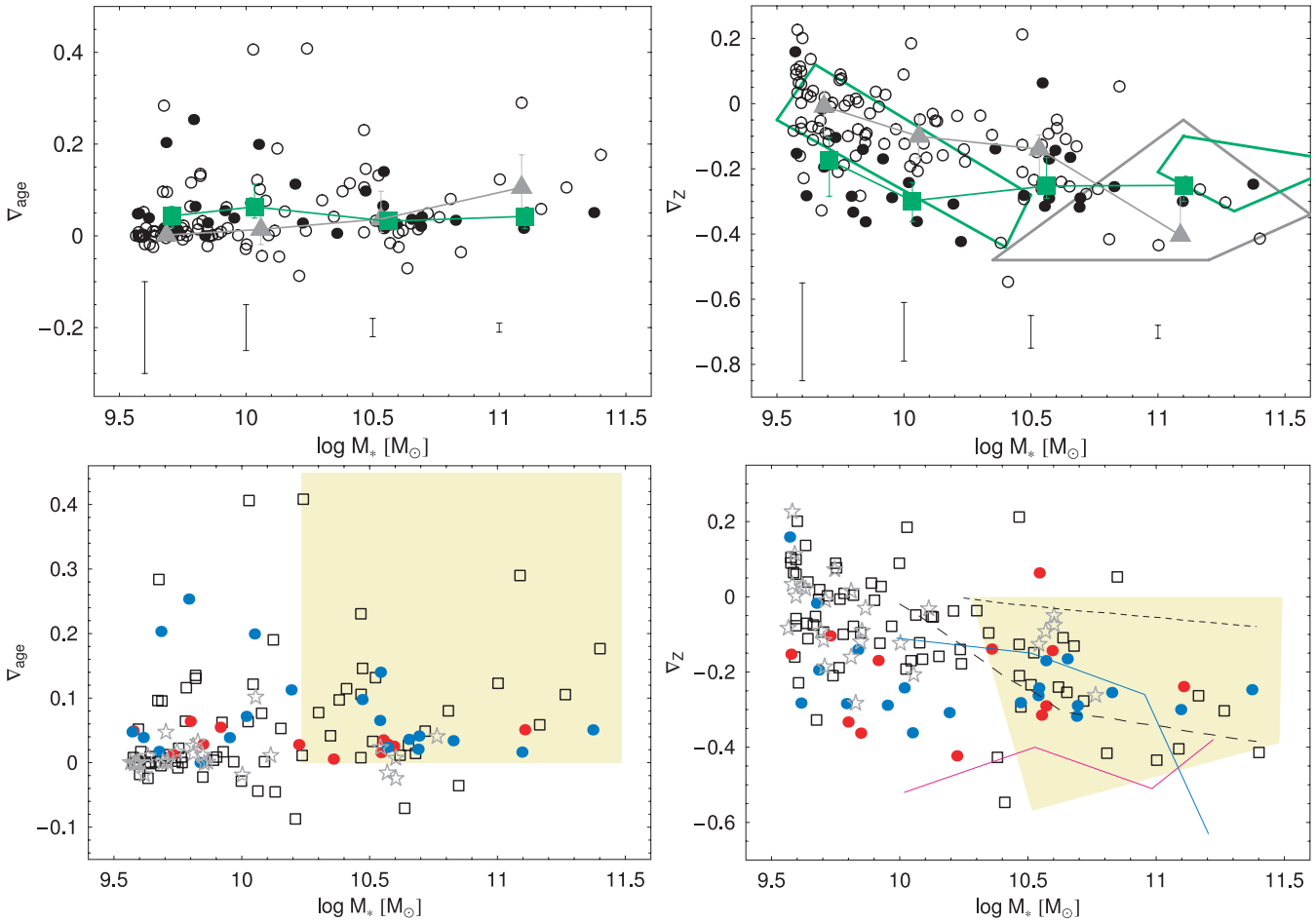

Figure 1. Age (left-hand panels) and metallicity (right-hand panels) gradients as a function of stellar mass (assuming an AY IMF). Top panels: black filled and black open circles are for cluster and group members. The lines connected by grey triangles and green boxes are the medians for groups and clusters, respectively. The error bars are the quartiles of sample distribution in each mass bin. At the bottom of the panels we also show the uncertainties on galaxies at different stellar masses, shown as error bars and determined as described in the text. On the right-hand panel we also show the results from local cluster (green thick lines) and groups (grey thick lines) galaxies in Spolaor et al. (2009), the polygonals bound the regions where these data are distributed. Bottom panels: black open boxes, grey open stars, red and blue points are for galaxies in normal and fossil groups, inner and external regions of clusters, respectively. Our results are compared with findings from other simulations. The predicted metallicity gradients from dissipative collapse model in Kawata & Gibson (2003) and those from merging in Bekki & Shioya (1999) are shown as long- and short-dashed lines. The shaded region is for remnants of major merging between gas-rich disc galaxies in Hopkins et al. (2009). Blue and pink lines are the results from the chemodynamical model in Kawata (2001), respectively, for strong and weak SN feedback.

gradients. However, a cloud of high age gradients in galaxies with $\log M_*/\mathrm{M}_\odot \lesssim 10.5$ is found in the external regions of simulated clusters and in normal groups, while galaxies in cluster cores and fossil groups have a quite tight distribution around $\nabla_{\rm age} \lesssim 0.05$ (see bottom panels). This is an interesting hint of the effect of the environment on the low-mass systems, acting on flattening age gradients in higher density regions. Moreover, in terms of average quantities, galaxies in the groups have shallower gradients, when compared with clusters. In particular, FG galaxies are distributed along a tighter sequence in both the age and the metallicity gradients.

At higher masses we have found slightly positive age gradients and negative metallicity gradients. On the side of the most massive galaxies ($\log M_*/\mathrm{M}_\odot \gtrsim 10.7$), the mean age gradients become increasingly positive with mass at the high-mass end; on the contrary, the trend of metallicity gradients at high masses gets flatter with mass. At these mass scales (normal) group galaxies show higher positive age gradients and steeper negative metallicity gradients. In particular, while groups present a continuous steepening of metallicity gradients with mass, the mass trend of cluster members turns from steep to flat at around $\log M_*/\mathrm{M}_\odot \sim 10.3$–$10.4$, to slightly increasing thence on.

Such trend inversion in the slope of metallicity gradients is corroborated by comparing with data from a sample of cluster and group galaxies collected in Spolaor et al. 2009 (see also T+09) and shown in the top right-hand panel of Fig. 1. Although their low-mass region is populated by cluster galaxies only, at the massive side cluster galaxies have shallower metallicity gradients than the ones in group galaxies, qualitatively confirming our trends. The slope of the massive side is even steeper with mass than ours, probably and partially due to a dearth of very massive galaxies in our simulated sample (Romeo, Portinari & Sommer-Larsen 2005), apart of the BCGs. Likewise, our cluster data follow a less steep trend than theirs at the low-mass side too.

As shown from the error bars in the upper panels of Fig. 1, the estimated gradients in low-mass systems are intrinsically noisier than the ones for massive galaxies. The error bars give an

estimate of the uncertainty in the gradients and contribute to the scatter in the derived trends with stellar mass. See Appendix A2 for further details about the procedure performed to obtain such results.

In the same Fig. 1 we add a comparison with other models as well, mostly from high-resolution hydrodynamical simulations of disc mergers (Bekki & Shioya 1999; Hopkins et al. 2009). In particular, the Z gradients of massive systems fall in the range covered by merger remnants in Hopkins et al. (2009). Our trend for metallicity gradients is also qualitatively consistent with the prediction of the chemodynamical model by Kawata & Gibson (2003). Instead, our results are quite inconsistent with the almost flat gradients derived from merging model in Bekki & Shioya (1999). Finally, when comparing with simulations in Kawata (2001), we note that our points at intermediate mass are placed along their curve derived from models with strong stellar feedback, at least till 10^{11} $M_{\odot}$. To this regard, in the discussion below we will come back upon the role of SN winds in shaping the trend of Z gradients with mass.

To check the dependence on other parameters than stellar mass, in Fig. 2 we discuss the trends in Fig. 1 by splitting the sample in two classes of galaxy colours, specific star formation rate (SSFR) over the last Gyr (SSFR $=$ SFR$/M_*$) and velocity dispersion. At $\log M_* \lesssim 10.5$ the bluest galaxies have the highest (positive) metallicity gradients, while this result is inverted for massive galaxies. The age gradients do not show particular trends. In terms of SSFR, only few galaxies are star forming at $z = 0$ (see R+08), and mostly the more massive ones in groups; these have positive age gradients and the steepest negative metallicity gradients. Note that few of the most massive galaxies (with $\log M_*/M_{\odot} \gtrsim 10.7$) in our sample, with a recent star formation history ($\log$ SSFR > -2) and bluer colours ($B - V < 0.8$), present steep age and metallicity gradients and are likely candidate for late-type systems. Merging and SN feedback alone do not allow these systems to move on to the red sequence, requiring the inclusion of other sources of feedback (e.g. AGN feedback) to quench SF and flatten the gradients. Finally, we also analyse the effect of a cut in velocity dispersion: due to the tight correlation with stellar mass, the systems affected by this criterion are predominantly low-mass systems in groups.

In Fig. 3, galaxies are classified by their values of central metallicity and age. We confirm that both metallicity and age gradients depend on central quantities (e.g. Hopkins et al. 2009; Rawle et al. 2010; T+10). In particular, metallicity gradients strongly depend on the central metallicity, with metal-poor systems having higher values (null or positive). In the last panels, we can also report a substantial agreement between the simulations and the median gradients recovered from local ETGs in T+10 (black symbols in the right-hand panels of Fig. 3). As found in T+10, here we can see that metallicity and age gradients are strong functions of central age: massive and older systems have null age gradients and shallower metallicity gradients (~ -0.2, -0.3). This is quite in agreement with other observations (e.g. Spolaor et al. 2009; Rawle et al. 2010) and simulations of massive merger remnants discussed above (Bekki & Shioya 1999; Kobayashi 2004; Hopkins et al. 2009). On the other hand, the agreement between observed and simulated younger galaxies is looser, what might be tracked to the absence of those field galaxies in the simulated sample that are expected to have steeper gradients (La Barbera et al. 2005; Tortora et al. 2010).

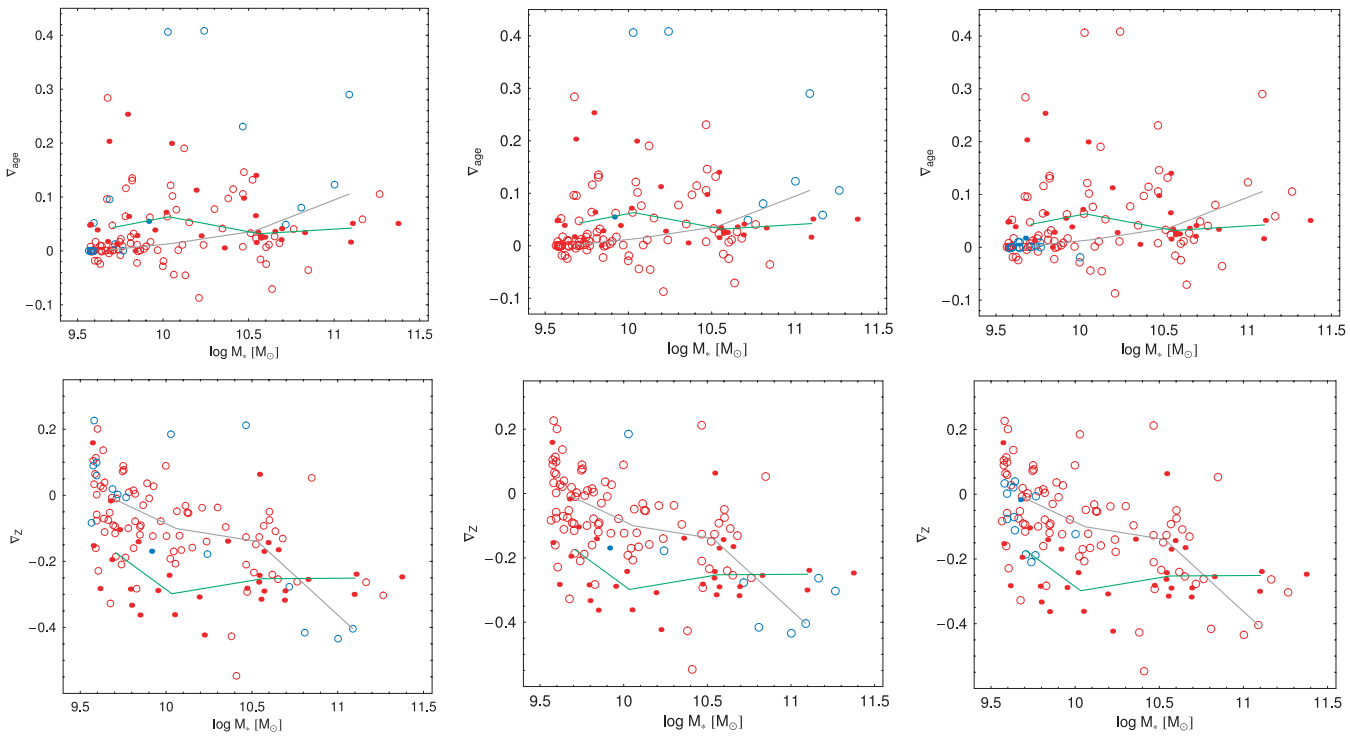

Figure 2. Age (top panels) and metallicity (bottom panels) gradients as a function of stellar mass. Filled and open symbols are for cluster and group galaxies, respectively. Grey and green lines are the medians for groups and clusters. From the left to right we divide galaxies in bins of total colour $B - V$, specific star formation SSFR and velocity dispersion. First panels: red and blue symbols are for galaxies redder and bluer than $B - V = 0.8$. Second panels: red and blue symbols are for galaxies with log SSFR lower and higher than -2. Third panels: red and blue symbols are for a total velocity dispersion higher and lower than 150 km s^{-1}, respectively.

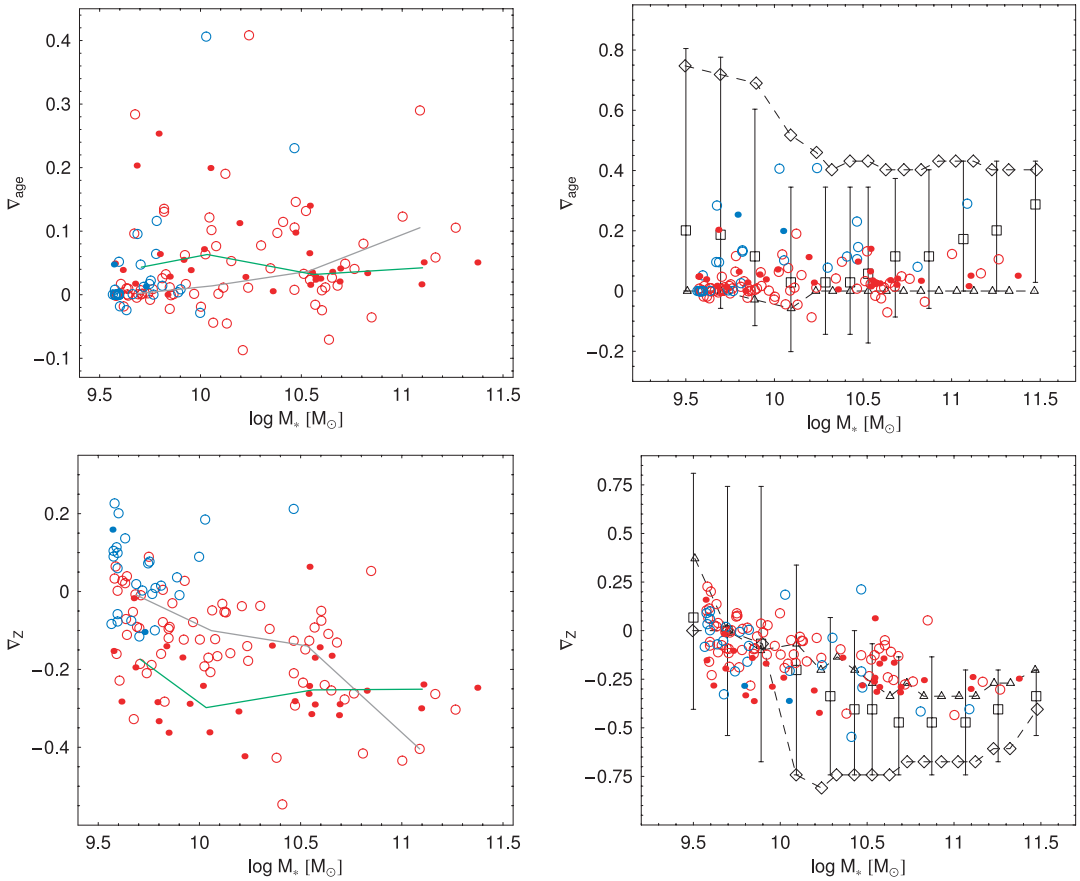

Figure 3. Age (top panels) and metallicity (bottom panels) gradients as a function of stellar mass. Filled and open symbols are for cluster and group galaxies, respectively. Grey and green lines are the medians for groups and clusters. From the left to right we divide galaxies in bins of central metallicity and age. Left-hand panels: red and blue symbols are for galaxies more and less metal rich than 0.008 at their centre. Right-hand panels: red and blue symbols are for galaxies centrally older and younger than 6 Gyr. Here, we compare with results from the analysis of the local sample of ETGs in T+10 [where the Chabrier (2001) IMF is suitably converted to an AY one]. The boxes with bars are the results for all the sample, while the squares and triangles are for galaxies with a central age <6 and >6 Gyr, respectively.

4 DISCUSSION

The net result of the observed quantities at $z = 0$ is the reflection of all the physical processes modelled in the simulation code (namely radiative cooling, stellar winds, SN feedback and galaxy merging) and represents the endpoint of galaxy evolution along the cosmic history. The next step would be the investigation of the evolution of the population gradients with redshift, which will be the topic of a forthcoming paper. Even at this stage though, we can build a clear picture of the relative contributions of each physical process in shaping the present day trends.

The overall trend of metallicity gradients with mass is only partially consistent with the expectation from a monolithic collapse, where the accretion of SSPs produces a higher central metallicity and negative metallicity gradients, that are steeper at larger masses where the potential well is deeper.

At high masses, the null age gradients are the consequence of galaxy merging that produces a mixing of the SSPs after the event. The null gradients are in fact more common in cluster environment and contrast with the presence of positive gradients in (normal) group environment (see e.g. Fig. 1), where there are still a few massive star-forming massive systems (Fig. 2).

The 'merging remnant' systems are also the ones having the shallower (negative) metallicity gradients with respect to the steeper ones of the star-forming systems. This shows that at the massive side merging is still a major player of the galaxy evolution – what makes our results consistent with former simulations of galaxy mergers (see Fig. 1).

In fact, typically major dry mergers are known to level out pre-existing metallicity and colour gradients (see Di Matteo et al. 2009; Pipino et al. 2010), hence this feature imposes a constraint upon the relevance of merging over passive evolution at the high-mass end. In particular, at the highest masses the occurrence of strong mass accretion due to minor and, mainly, major merging prevents the gradients to further steepen.

At these mass scales, the amount of energy ejected by SNe contributes to yield steep Z gradients in massive star-forming galaxies, which still have to experience major merging events. On the other mass side (i.e. $\log M_*/M_\odot < 10$) instead, SNe produce, on average, null gradients due to the large meshing action required by winds easily propagating within their smaller volume and less deep potential wells. In this case we see that star formation has been shut off in all classes of galaxies (Fig. 2), and the age gradients are similarly close to zero. Environment acts as to make galaxies in clusters have negative gradients with respect to the groups. This suggests a different response of the enriched medium against SNe explosions. In lower density environments, the metals are kept in the small systems and recycled until the overall metallicity gradients are swept

out, while in the cluster core environment the higher density and the more numerous encounters imply that part of the metals is lost in the IGM and the net metallicity gradients stay negative as for massive systems.

However, there are a number of galaxies (both in cluster outskirts and groups) which seem to diverge from the overall age trend at the low-mass end, since they show positive age gradients but metallicity gradients consistent with the averages of the sample. These systems do not correlate with other galaxy properties, like the star formation, colour or velocity dispersion (see e.g. Fig. 2). Instead they are the systems with lower ages (see Fig. 3), well matching the suggestion that age is responsible of the scatter of the gradients (especially the age ones) in the observed systems (see T+10 and Fig. 3). These are systems that have born in the late epochs and that have evolved quite passively so far without experiencing any other stellar processes but stellar ageing. We have checked that these galaxies are gently migrating toward the zero gradients which they will reach in the near future. Most of these dwarf-like systems resulted to be star forming at $z > 0$ (R+08) and are now dead mainly as a consequence of their interaction with close companions (as demonstrated by the fact that the few star-forming galaxies are in normal groups and cluster outskirts), while SNe seem not to play a major role. At the same time these systems could not be residing in FG and inner cluster regions because they had merged at earlier epochs on to the BCGs.

5 CONCLUSIONS

In this paper, we have used the *N*-body+hydrodynamical simulations described in R+08 to study the age and metallicity gradients in galaxies as functions of mass in the range $\log M_*/\mathrm{M}_\odot \in (9.5$–$11.5)$ and environment (from groups to cluster centres). Our results show different trends of age and metallicity gradients with mass and galactic environment at $z = 0$. With respect to the mass (1) dwarf galaxies have generally null age gradients and shallower or null metallicity gradients (with few cases of positive age gradients); (2) massive early types ($\log M_*/\mathrm{M}_\odot \sim 10.5$) have moderate age gradients that slightly increase with mass, and negative metallicity gradients (~ -0.2, -0.3, see e.g. Rawle et al. 2010; T+10), which reach the steepest values ~ -0.4 in few of the most massive galaxies ($\log M_* \gtrsim 10.5$). At fixed stellar mass there is a clear dependence on the central galaxy age, since younger galaxies have positive age gradients and slightly steeper Z gradients, and central metallicity. Similarly, some marginal trends are found as a function of SSFR and colour: in particular the very massive systems with bluer colours and active SF are found to have steeper gradients. This mass separation in the profile slope is in agreement with other models (e.g. Kawata 2001; Kawata & Gibson 2003; Hopkins et al. 2009), and observations (Spolaor et al. 2009; Rawle et al. 2010; T+10), even though the statistic for our very massive side is quite poor.

Such behaviour can be explained in terms of the different role played by merging. At $\log M_*/\mathrm{M}_\odot \lesssim 10.5$ mergers are rare and thus less effective in mixing stellar population (e.g. de Lucia et al. 2006); then the only physical mechanisms in action are the SN feedback and the passive ageing (similarly to a monolithic collapse scenario), that result into the decreasing trend of Z gradients (see also Kawata & Gibson 2003; Pipino et al. 2010).

On the other side, the flattening of metallicity gradients trend at larger masses can be due to the higher frequency of major dry mergers at low redshift, which have an increased efficiency in producing flatter metallicity profiles. Pipino et al. (2010) have demonstrated that equal mass dry mergers between ellipticals systematically halve the slope of any pre-existing metallicity gradient.

With respect to the environment, systems with positive age gradients tend to be found in the external parts of clusters and in groups, *independently of galaxy's mass* and with a quite large spread; while galaxies in the cluster cores and fossil groups have, on average, quasi-null age gradients, again at all masses. However, when analysing the average values, cluster dwarf galaxies have steeper metallicity gradients with respect to the ones in groups, which also present shallower values more peaked around zero (with a larger fraction of positive gradients); slight steeper age gradients are observed in cluster galaxies too. At very high mass, albeit the lower statistics, this trend gets inverted and galaxies in groups have steeper (negative) metallicity gradients (La Barbera et al. 2005). As to the scatter of the relations, cluster cores and FGs present the tightest distribution of age gradients, while the metallicity gradients show no strong differences in the scatter among the different environments.

Therefore, besides the main role of SN feedback, we have found that environment shapes differently the gradients at low and high masses. At low masses, tidal interactions are acting to give steeper metallicity gradients in cluster galaxies, while merging produces shallower gradients in massive systems in the same environment.

In forthcoming works, we plan to extend this analysis to higher z and as well to the BCGs, to put on a firmer ground our physical interpretations. In particular, we aim at further investigating the physical processes that rule the very massive galaxies such as galaxy major merging and AGN feedback (Antonuccio-Delogu & Silk 2008; Tortora et al. 2009), which would be important to shape both the global properties and the gradients in stellar populations.

ACKNOWLEDGMENTS

We thank the anonymous referee for the suggestions which helped to improve the paper. CT was funded by the Swiss National Science Foundation. ADR acknowledges support from ALMA-CONICYT FUND through grant 31070023, from FONDECYT – Proyecto de Iniciación a la Investigación No. 11090389 and from UNAB – Proyecto Regular No. DI-35-09/R. AM acknowledges partial support from Proyecto Regular de Investigacion UNAB DI-41-10/R.

REFERENCES

Antonuccio-Delogu V., Silk J., 2008, MNRAS, 389, 1750
Antonuccio-Delogu V., Becciani U., Ferro D., Romeo A., 2003, Mem. Soc. Astron. Ital. Suppl., 1, 109
Arimoto N., Yoshii Y., 1987, A&A, 173, 23 (AY)
Bekki K., Shioya Y., 1999, ApJ, 513, 108
Benson A. J., Pearce F. R., Frenk C. S., Baugh C. M., Jenkins A., 2001, MNRAS, 320, 261
Carlberg R. G., 1984, ApJ, 286, 403
Chabrier G., 2001, ApJ, 554, 1274
Davies R. L., Sadler E. M., Peletier R. F., 1993, MNRAS, 262, 650
de Lucia G., Springel V., White S. D. M., Croton D., Kauffmann G., 2006, MNRAS, 366, 499
di Matteo P., Pipino A., Lehnert M. D., Combes F., Semelin B., 2009, A&A, 499, 427
Forbes D. A., Sánchez-Blázquez P., Proctor R., 2005, MNRAS, 361, 6
Helly J. C., Cole S., Frenk C. S., Baugh C. M., Benson A., Lacey C., Pearce F. R., 2003, MNRAS, 338, 913
Hopkins P. F., Cox T. J., Dutta S. N., Hernquist L., Kormendy J., Lauer T. R., 2009, ApJS, 181, 135

Kawata D., 2001, ApJ, 558, 598
Kawata D., Gibson B. K., 2003, MNRAS, 340, 908
Kobayashi C., 2004, MNRAS, 347, 740
Kobayashi C., Arimoto N., 1999, ApJ, 527, 573
La Barbera F., deCarvalho R. R., Gal R. R., Busarello G., Merluzzi P., Capaccioli M., Djorgovski S. G., 2005, ApJ, 626, 19
Larson R. B., 1974, MNRAS, 166, 585
Larson R. B., 1975, MNRAS, 173, 671
Peletier R. F., Davies R. L., Illingworth G. D., Davis L. E., Cawson M., 1990a, AJ, 100, 1091
Peletier R. F., Valentijn E. A., Jameson R. F., 1990b, A&A, 233, 62
Peletier R. F. et al., 2007, MNRAS, 379, 445
Pipino A., D'Ercole A., Matteucci F., 2008, A&A, 484, 679
Pipino A., D'Ercole A., Chiappini C., Matteucci F., 2010, 407, 1347
Rawle T. D., Smith R. J., Lucey J. R., 2010, MNRAS, 401, 852
Romeo A. D., Portinari L., Sommer-Larsen J., 2005, MNRAS, 361, 983
Romeo A. D., Sommer-Larsen J., Portinari L., Antonuccio-Delogu V., 2006, MNRAS, 371, 548
Romeo A. D., Napolitano N. R., Covone G., Sommer-Larsen J., Antonuccio-Delogu V., Capaccioli M., 2008, MNRAS, 389, 13 (R+08)
Sijacki D., Springel V., Di Matteo T., Hernquist L., 2007, MNRAS, 380, 877
Spolaor M., Proctor R. N., Forbes D. A., Couch W. J., 2009, ApJ, 691, 138
Tamura N., Ohta K., 2000, AJ, 120, 533
Tamura N., Ohta K., 2003, AJ, 126, 596
Tamura N., Kobayashi C., Arimoto N., Kodama T., Ohta K., 2000, AJ, 119, 2134
Tortora C., Napolitano N. R., Romanowsky A. J., Capaccioli M., Covone G., 2009, MNRAS, 396, 61
Tortora C., Napolitano N. R., Cardone V. F., Capaccioli M., Jetzer Ph., Molinaro R., 2010, MNRAS, 407, 144

APPENDIX A: SYSTEMATICS

In this section we will analyse various systematics induced by selection criteria and the fit procedure adopted to derive the age and metallicity gradients.

A1 Fitting procedure

As described in the text, we have performed a linear fit $\log X - \log R$ in order to recover the age and metallicity profiles of the simulated galaxies. The first basic step of such a procedure is to derive the galaxy centre from the distribution of the star particles. The particle distributions for two template galaxies are shown in Fig. A1. The choice of the median as the galaxy centre is dictated by the scarce sensitivity of such estimator to the outliers: in many cases indeed, the particle distribution is not symmetric (as shown in the bottom panel of Fig. A1), therefore, the median is more suitable to determine the minimum of the potential well.

The profiles for galaxy age and metallicity are shown in Fig. A1 too. The data points are compared with our best-fitted profile, isodensity contours and medians in different radial bins. The fitting procedure is directly performed on the collection of points, cutting the tails of age and metallicity distributions out of 3σ, to avoid systematics from outliers affecting the slope's estimate.

Finally, we have also analysed the change in the derived gradients when the age and metallicity profiles are fitted in a limited radial range, as made with observations. We fit the profiles using only the particles in the range $(R_{\rm eff}/10, R_{\rm eff})$, where $R_{\rm eff}$ is the radius

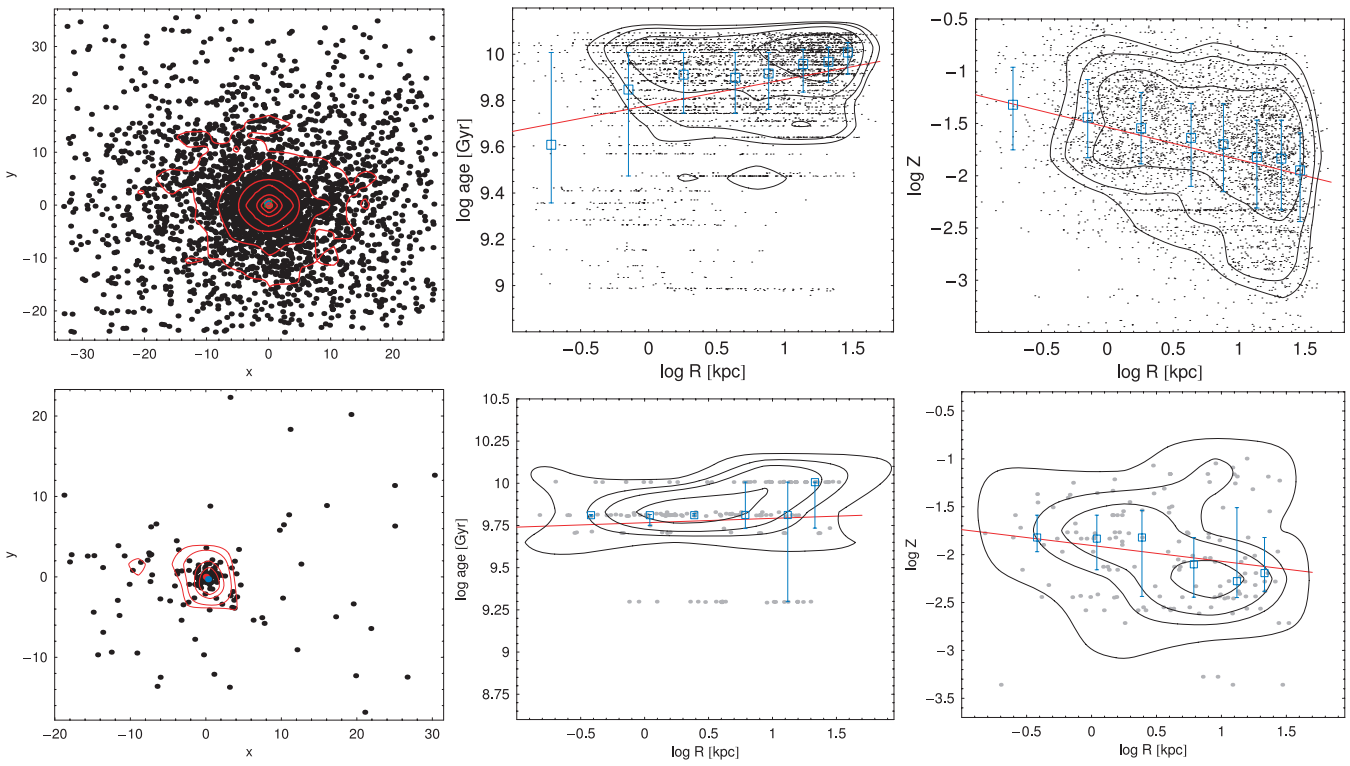

Figure A1. Particle distributions, age and metallicity profiles from the left to right, for a massive (top panels) and dwarf (bottom panels) group galaxy. Left-hand panels: distribution of particles in the plane x–y. The axes coordinates are renormalized to the median of the particles (red point), while the blue point is the mean. The red contours show the density of data points. Middle panels: galaxy age profile shown as log age versus log R, the contours show the density of data points, the blue bars are the medians with the 25–75th percentiles, while the red line is the linear fit we have performed. Right-hand panels: the same as the middle panels but for the metallicity profile.

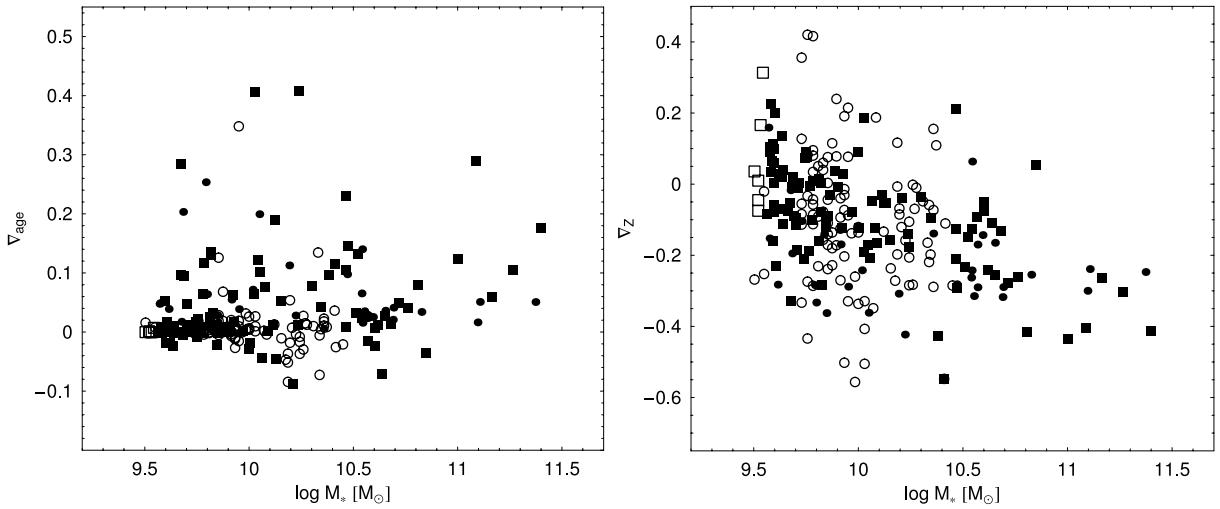

Figure A2. Age (left-hand panel) and metallicity (right-hand panel) gradients as a function of stellar mass. Circles and boxes are for cluster and group members, respectively. Filled and open symbols are for galaxies with $N_{\rm par} > 80$ and ≤ 80, respectively.

which encloses half of the stellar mass, and the final results are qualitatively unchanged.

A2 Systematics induced by the small number of particles

We have performed a series of tests on our galaxies to understand what is the spurious scatter introduced in fitting objects with a very low number of particles. We have taken some galaxies with a high number of particles (in the range 1000–5000) and fixed the derived slopes as with a null uncertainty. Then we have extracted from them 1000 synthetic galaxies having a number of particles $N_{\rm par} = 70, 225, 710$ and when possible $= 2250$, which correspond, for the highest resolution in our simulations, to $\log M_* \sim 9.5, 10, 10.5$ and 11.5, respectively. The fitting procedure is performed on each of these 1000 synthetic systems and for each $N_{\rm par}$, from the slopes hence obtained we have derived a best median value and a 1σ uncertainty. While the best fitted slope of the original galaxies is perfectly recovered, with an almost null scatter, the uncertainty is not negligible and is, obviously, larger for very low mass systems, while is very small for the most massive galaxies with $\log M_* \sim 11$. We have presented these results in Fig. 1.

As already discussed, this uncertainty can produce part of the larger scatter observed in the gradients at very low masses and these systematics could be stronger when the number of particles is lower than the minimum value of 80 we have imposed. To understand the impact on our results, in Fig. A2 we show the age and metallicity gradients for both group and cluster members as a function of mass, classifying them on the basis of the number of particles. The cluster members are the systems strongly affected by our selection criterion on $N_{\rm par}$ that cuts out many galaxies with $\log M_* \lesssim 10.5$. Such a cut reduces the spread in the metallicity gradients, while for the age gradients no relevant variations are reported.

A3 Effect of the softening length

The softening length (s.l.) of our simulations is comparable to typical scales of the smallest galaxies ($\sim 1-2$ kpc, see e.g. Fig. A1) where it affects the spatial and velocity distribution of SPH particles (not their intrinsic age and Z). Our analysis is insensitive to the dynamical range, but it can be affected by the radial distribution of the particles. For this reason we have adopted the same self-consistency check of Appendix A2 to evaluate whether the particle density profile might produce a systematic variation of the gradient estimates. We have extracted from three of the intermediate massive galaxies ($N_{\rm par} \sim (900, 700, 600)$) a smaller number of particles ($N_{\rm par} \sim 100$) randomly following two extreme Sersic density profiles, with $n = 6$ and $n = 1$ respectively. To fully simulate a dwarf–like system, our random Montecarlo extractions were done assuming a smaller effective radius ($R_e \sim$s.l.) with respect to the original simulated galaxy. We have generated 100 Montecarlo extractions and derived the distribution of age and Z gradients for the two (extreme) Sersic indexes. For the $n = 6$ case we have obtained $\nabla_{\rm age} = (-0.001, 0.16, 0.07)$ and $\nabla_z = (-0.10, -0.23, 0.18)$ for the three groups of extractions, and for $n = 1$ we have obtained $\nabla_{\rm age} = (-0.009, 0.17, 0.02)$ and $\nabla_z = (-0.19, -0.13, 0.17)$ which are consistent within the typical statistical errors (e.g. see Fig. 1). We conclude that the s.l. has no systematic effects on the radial gradient estimates of small systems as it turned out to be only mildly sensitive to the intrinsic shape of the radial distribution of SPH particles.

This paper has been typeset from a TEX/LATEX file prepared by the author.